

# Process Design for Electromagnetic Forming of Magnesium Alloy AZ31 Using FE Simulation

**E. Uhlmann, L. Prasol\*, H. Roehrs**

Institute of Machine Tools and Factory Management, TU Berlin University, Germany

\*Corresponding author. Email: prasol@iwf.tu-berlin.de

## Abstract

*Magnesium wrought alloys are outstanding lightweight materials due to their low density and high specific strength. The low formability of magnesium wrought alloy AZ31 at room temperature is increased by electromagnetic forming in comparison to quasi-static forming. For a detailed study of electro-magnetic process a coupled FE simulation must be performed. In this paper the process design for electromagnetic forming of magnesium wrought alloy AZ1 using FE simulation is presented.*

*The complexity of an electromagnetic forming process requires the illustration of magnetic, thermal and structural dynamic domains. Moreover, it is also necessary to illustrate the electromagnetic resonant circuit RLC. Short processing time and the strong dependence of the physical domains to each other requires a coupled FE simulation.*

*The illustration of resonant circuit and the resulting formation of magnetic field is carried out in two-dimensional rotationally symmetric model in ANSYS MAPDL using a suitable material model. As a result time-dependent and location-dependent eddy currents and Lorentz forces are estimated.*

*Subsequently, the transmission of the estimated Lorentz forces and joule heat generation rates to ANSYS LS-DYNA is done. Due to the rotational symmetry of 2D ANSYS MAPDL model a transformation of the loads on 3D structures can be realized. The formation of an optimum deformation of a work piece in dependence of a defined die has been carried out. Here, the influence of different coil designs, die materials and geometries and RLC parameters was investigated.*

## Keywords

Electromagnetic forming, FE simulation, Magnesium wrought alloy AZ31

## 1 Introduction

The idea of using the power of pulse magnetic fields was introduced in the year 1958 when the first patent for an application of electromagnetic advices was presented in the United States of America. Since 1990s interest on electromagnetic forming has been increasing due to rising demands on flexibility, efficiency and sustainability of industrial production processes and products (Hahn, 2004). Electromagnetic forming processes can contribute an important part to meet the requirements mentioned above as they provide advantages in comparison to conventional processes (Psyk et al., 2011):

- Forming process is realized without any mechanical contact of work piece surfaces,
- Scrap minimization is a result of very high process repeatability,
- Short process  $t_p$  time enables high production rates and
- Electromagnetic forming processes can be realized without lubricants, whereby the environmental impact and sustainability increase.

It is also crucial that process conditions of electromagnetic forming modify mechanical behaviour of various materials. In particular, the formability of lightweight material magnesium alloy AZ31 is increased considerably by high strain rates (Ulacia et al, 2009; Ulacia et al., 2011, Feng et al., 2014, Uhlmann et al., 2014, Ahmad and Shu, 2015). These advantages are faced with a high process complexity due to numerous, interdependent factors. Without process simulation the interpretation of an electromagnetic forming process is dependent on time-intensive process design (Azab et al., 2003).

Process design of an electromagnetic forming process for a defined component is presented within this paper. Main aspects of this paper are

- Development of an appropriate simulation model,
- Design of manufacturing process for a complex component and
- Evaluation of electromagnetic forming process for a complex component made of magnesium alloy AZ31.

## 2 State Of Art

### 2.1 Electromagnetic Forming

Electromagnetic forming includes all production methods using the dynamic effect of a pulsed magnetic field directly for machining of a work piece (Neubauer et al., 1988). The duration of the magnetic pulse is only a few microseconds. The effect of the forming process occurs due to the inertia of the work piece with a time offset, but the energy conversion occurs abruptly. Therefore, electromagnetic forming is classified as method of high speed forming (Lange, 1993).

Electromagnetic forming is based on the physical effect of induction. The required energy for the forming process is stored in capacitors by charging them to a high voltage  $U$ . By discharging the capacitors over a high-current switch, the arising large currents  $I(t)$  generate an intense magnetic field  $H(t)$  outside the tool coil with the magnetic flux density  $B = \mu H$ . This magnetic field  $H(t)$  induces eddy currents  $I_{eddy}(t)$  in the work piece which are

running in the opposite direction compared to the primary currents  $I(t)$  in the tool coil (Lange, 1993, Finkenstein, von, 1967).

Due to the short process time  $t_p$  and high frequencies  $f$  of the discharging process the induced eddy currents  $I_{eddy}(t)$  are running near the surface of the sheet metal. It's justified by the skin effect. Consequently, the resulting Lorentz forces  $F_L(t)$  which depend on the primary magnetic field  $H(t)$  are acting for a short time  $t_p$  of 50 to 100  $\mu\text{s}$  on the work piece. The acting Lorentz  $F_L(t)$  forces are converted as a magnetic pressure on the work piece surface (Winkler, 1993).

## 2.2 Process Dependent Mechanical Behaviour of Magnesium Alloy AZ31

Material which is machined by electromagnetic forming is subjected with strain rates up to  $10^4 \text{ s}^{-1}$  and different mechanical stress states. Additionally, a local temperature increase is observed within the workpiece as a result of resistance heating and forming temperature due to the adiabatic character of the electro-magnetic process (Psyk et al., 2011). Within the framework of scientific studies the influence of different parameters at different loading conditions was investigated in detail (Ulacia et al., 2010, Ulacia et al., 2011, Feng et al., 2014, Ahmad and Shu, 2015, Kurukuri et al., 2015). In particular, the influence of strain rates in the range of  $10^{-4}$  to  $10^4 \text{ s}^{-1}$  and work piece temperatures of 20 to  $400^\circ\text{C}$  at tensile and compression conditions were investigated. As a result the following statements with regard to the formability of Mg alloy AZ31 can be derived:

- Yield stress  $Y_f$  increases with increasing strain rates, i.e. magnesium alloy AZ31 exhibits positive strain rate sensitivity (Ulacia et al., 2011, Feng et al., 2014, Ahmad and Shu 2015, Kurukuri et al., 2015). Strain rate sensitivity is more pronounced at tension (Ulacia et al, 2010, Ahmad and Shu, 2014, Kurukuri et al., 2015).
- Hardening of AZ 31 depends on strain rates (Ulacia et al., 2011, Ahmad and Shu, 2014, Kurukuri et al., 2015)
- Strain rate sensitivity is temperature-dependent (Ulacia et al., 2011)
- Magnesium alloy AZ31 is anisotropic and exhibits a tensile-compression-asymmetry at room temperature. With increasing strain rates tensile-compression-asymmetry increases (Ulacia et al., 2012).
- Perpendicular anisotropy increases with increasing strain rates (Ulacia et al., 2011), while mechanical behaviour of planar anisotropy at high strain rates is not conclusive answered. ULACIA ET AL. exhibit an increase of planar anisotropy (Ulacia et al., 2010) while ULACIA ET AL. also shows a decrease (Ulacia et al., 2011) or influence of planar anisotropy by high strain rates (Kurukuri et al., 2015).

The dependence of strain rates on the yield stress  $Y_f$  can be described mathematically by a material model for thermo-viscoplastic behaviour. Cowper and Symonds (Cowper and Symonds, 1952), Perzyna (Perzyna, 1966), Johnson and Cook (Johnson and Cook, 1983) as well as Zerilli and Armstrong (Zerilli and Armstrong, 1985) suggest constitutive models for description of electromagnetic forming process assuming

isotropic hardening. The description of the tensile-compression-asymmetry can be realized using yield criterion of Cazacu (Cazacu et al., 2006).

### 2.3 Simulation of Electromagnetic Forming Process

The process behavior during electromagnetic forming can be described by electrodynamic, thermodynamic and continuum mechanical field equations using vector analysis (Azab et al, 2003, L'Eplattenier et al., 2008). The description of an electromagnetic forming process requires the mapping of a

- Circuit model (RLC resonant circuit),
- Electromagnetic model,
- Mechanical model and
- Optional thermal model.

The *circuit model* can be formulated by applying the 2<sup>nd</sup> KIRCHHOFF's law on the resulting equivalent circuit as an ordinary differential equation (Winkler, 1973). The *electromagnetic model* is based on the solution of the quasi-static approximation of MAXWELL's equations (L'Eplattenier, 2008). As a result of the electromagnetic model the estimated magnetic force density (Cao et al., 2015) is being transferred to the *mechanical model*. Here, the LORENTZ force  $F_L(t)$  acts as a body force and is integrated in the mechanical model in the momentum balance. The solution of the thermal model is based on the conservation of energy. By estimating the JOULE heating rate in the electromagnetic model and additionally the forming temperature within the work piece both quantities are being used for the *thermal model*.

The solution of the resulting differential equations is done by FE method. In particular, it has to be taken into account in which way the respective models are being coupled. In general, there are different types of model domains, i.e. which domains are being coupled. Furthermore, the coupling strategy is also important. There are four model domains:

1. Reduced models (only mechanical model),
2. Basic models (electrodynamic model and mechanical model),
3. Extended models (electrodynamic model, mechanical model and thermal model or circuit model) and
4. Extensive models (circuit model, electrodynamic model, mechanical model and thermal model).

The models of the category two up to four can be coupled via different strategies (Pérez et al., 2009). A distinction is made between *loose* coupling (estimation of electrodynamic domain for a defined number of steps and transfer as boundary condition to mechanical domain), *sequential* coupling (bilateral exchange of load data and state variables after each time step with an update of the domains) and *direct* coupling (field variables of different domains are solved simultaneously in a combined system of equations). *Reduced models* use only the mechanical domain to calculate displacements (Imbert et al., 2005, Wang et al., 2006). *Basic models* with a coupling of electrodynamic and mechanical models are presented by (Oliveira, 2005, Correira et al., 2008, Unger et al.,

2008) with a *loose coupling* and by (Mamalis et al., 2006) with a *sequential coupling*. *Extended models* are presented by (Meriched et al., 2000, Xu et al., 2015). *Extensive models* are presented by (Bessonov and Golovashchenko, 2006; Ulacia et al., 2008, Doley and Kore, 2014, Cao et al., 2015). Most of the presented papers deal with the investigation of aluminum. Only (Ulacia et al., 2008; Doley and Kore, 2014; Xu et al., 2015) take investigations of AZ31 into account.

### 3 Approach

In the context of this paper the approach in the process design for an electromagnetic forming process is presented for complex work piece made of magnesium alloy AZ31 at room temperature, **Fig. 1**. The complexity of an electromagnetic process thus requires in the first step, the conceptual design of an appropriate simulation model using an appropriate material model. The process design for an electromagnetic forming process for complex work piece geometry by varying the parameters

- tool coil geometry,
- die material and
- die geometry

concerning system parameters – capacity  $C$  and charging voltage  $U$  – is the aim of the investigation. The process-related potential of the electromagnetic forming process with respect to work piece feasibility is shown. The evaluation of the permissible material strength in the areas with maximum stress is based on experimentally determined reference values.

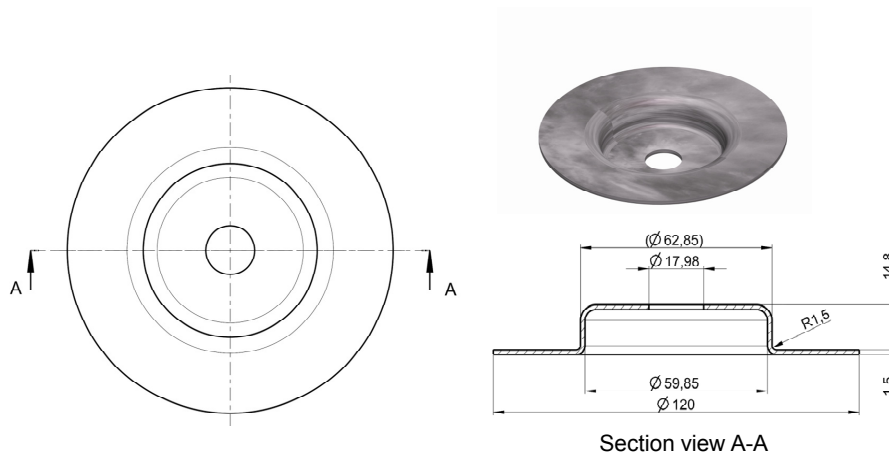


**Figure 1:** Anticipated work piece geometry

### 4 Simulation Concept

The simulation concept shown in **Fig. 2** was used to combine an accurate estimation of LORENTZ forces and JOULE heat generation rates – *implicit 2D* model – as well as an accurate deformation and dynamic behaviour of the work piece while interacting with the

die during the forming process – *explicit 3D* model. The PERZYNA model has been implemented in the implicit 2D simulation – domain *simplified mechanics*. The required parameter for the PERZYNA model has been adapted to temperature and strain rate dependent flow curves.

Flow curves have been experimentally determined by the Bundesanstalt fuer Materialpruefung und -forschung (BAM), Berlin, Germany. In the context of explicit 3D simulation the Johnson-Cook model with experimentally determined characteristics has been used in the domain Complex Mechanics (Feng et al., 2014).

The choice of different materials models, which have a minimal discrepancy between the determined deformations, is justified by the ANSYS structure and validation results. ANSYS MAPDL granted only the use of PERZYNA model as a strain rate dependent model. As part of the material model validation it has been shown that the experimentally determined parameters up to  $1000 \text{ s}^{-1}$  does not describe the material behaviour with sufficient accuracy. A rotationally symmetrical tool coil was used to validate the material model (Uhlmann and Prasol, 2013). Rather, the numerical results showed that strain rates up to  $2500 \text{ s}^{-1}$  occur during electromagnetic forming process. In the literature comparable material data up to strain rates of  $3000 \text{ s}^{-1}$  is presented by (Feng et al., 2015) for the JOHNSON-COOK model. Only ANSYS LS-DYNA granted the usage of JOHNSON-COOK model as a strain rate and temperature dependent material model.

A two-dimensional, rotationally symmetrical model is used in ANSYS MAPDL to determine the loads – Lorentz forces and Joule heating rates – within a forming process without a dominant die. A three-dimensional model in ANSYS LS-DYNA is used to simulate the deformation process within the die. Both models are coupled with a loose algorithm. Within the implicit 2D model the estimation of magnetic field  $H(t)$  and tool coil current  $I(t)$  is realized with a direct coupling of model blocks circuit and electromagnetic field. This results in the determination of parameters Lorentz force and Joule heating rate which are passed in each time step as boundary conditions to the model blocks simplified mechanics and simplified thermal field. The mesh morphing of the deformed work piece structure is performed simultaneously at each time step. Within implicit 2D model an accurate estimation of Lorentz forces is realized by estimation of inductance  $L$  in each time step. Due to the forming process a permanent change of inductance  $L$  occurs which has to be taken into account. Temperature dependence of material parameters is also taken into account.

In the explicit 3D model a transient structural mechanical simulation is done. Model block thermal field is directly coupled with model block complex mechanics which considers also Joule heating rates and deformation heating rates due to the adiabatic process. To enable this coupled thermal structural analysis defined keywords have to be add to LS-DYNA .k-file before solving.

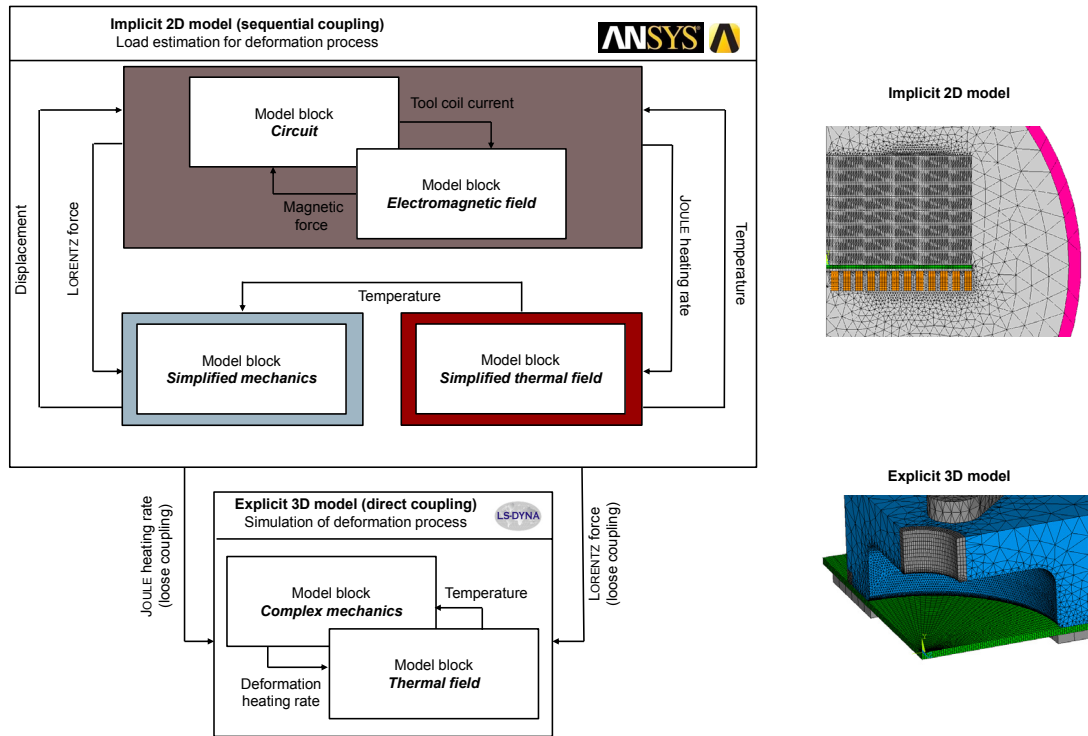


Figure 2: Schematic representation of the simulation concept

## 5 Results

Following, the presented results are based on preliminary investigations. In advance the tool coil geometry, the die material and the blank holder force has been optimized. The adapted tool coil geometry is shown in **Fig. 3**.

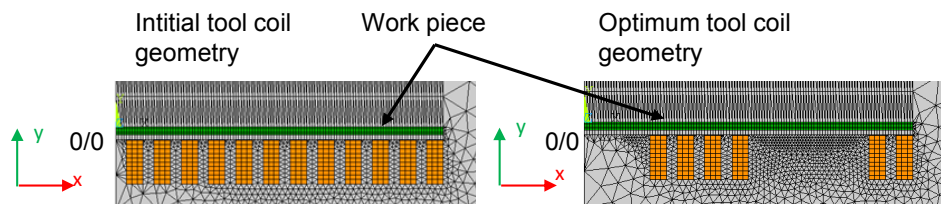


Figure 3: Optimum tool coil geometry

Steel has been found to be optimum material due to its mechanical properties. Depending on the provided charging energy  $E$  and the charging voltage  $U$  arising optimum blank holder pressures has been identified. The blank holder pressures can be found in the following charts **Fig. 4** to **Fig 8**.

In dependence of the die height  $h$  it is possible to realize a work piece contour which aims the contour of the work piece shown in **Fig. 1**. The percentage values given in **Fig. 4** and **Fig. 8** describe the degree of die filling, estimated as the ratio of the numerical integrals of the curves for actual and desired contour (**Fig. 1**) in the portion between  $r = 8.99$  mm and  $r = 35$  mm. Basically, a decrease of the die height causes an increase in the desired work piece geometry.

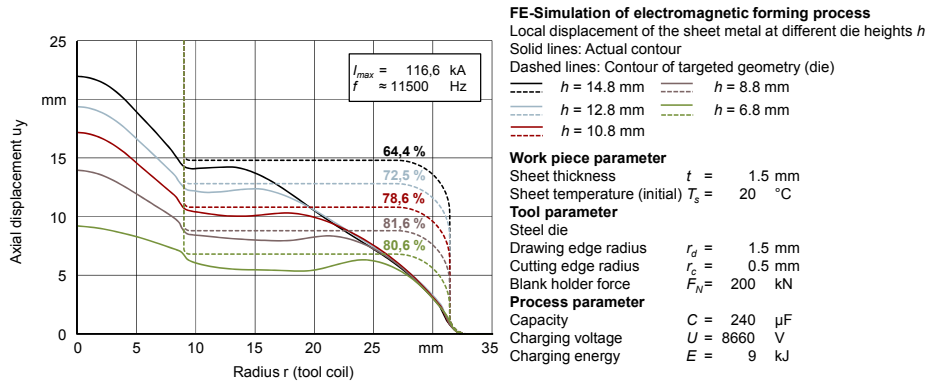


Figure 4: Displacement  $u_y$  for different die heights  $h$  (simulation time = 300  $\mu$ s)

The principle strain  $\varphi_I$  limits the maximum material stress in the plane strain condition. Due to instability of the membrane this condition is located in the region of the drawing edge  $r_d$  and the cutting edge  $r_c$ . The dependence of  $r_d$  is shown in Fig. 5. The cutting edge  $r_c$  is constant  $r_c = 0.5$  mm. Increasing drawing edge  $r_d$  causes a decrease in the principal strain. Due to this an increasing material stability in this area is expected. The cutting edge  $r_c = 0.5$  mm causes material failure due to the high principle strain. In general instability of membrane causes material failure during electromagnetic processes (Uhlmann and Scholz, 2003).

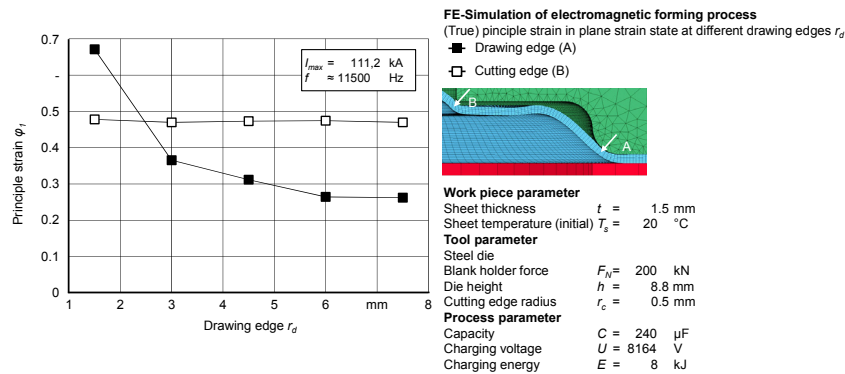


Figure 5: Principle strain  $\varphi_I$  in dependence of drawing edge  $r_d$  ( $r_c$  is constant)

Fig. 6 shows the secure (true) principle strains  $\varphi_I$  measured by electromagnetic forming. For the investigations the experimental setup presented by (Uhlmann and Prasol, 2014) has been used. Due to the uniform force effect on the forming area and instability of membrane (drawing edge, cutting edge) the influence of electromagnetic forming on the maximum allowable principle strains in the material can be investigated.

The comparison of the numerically determined (true) principle strains  $\varphi_I$  in the area of the drawing edge radius  $r_d$  (Fig. 5) with the experimentally determined (true) principle strains  $\varphi_I$  (Fig. 6) shows an exceed of permissible (true) principle strains  $\varphi_I$  at the determined current values  $I_{max}(t)$ .



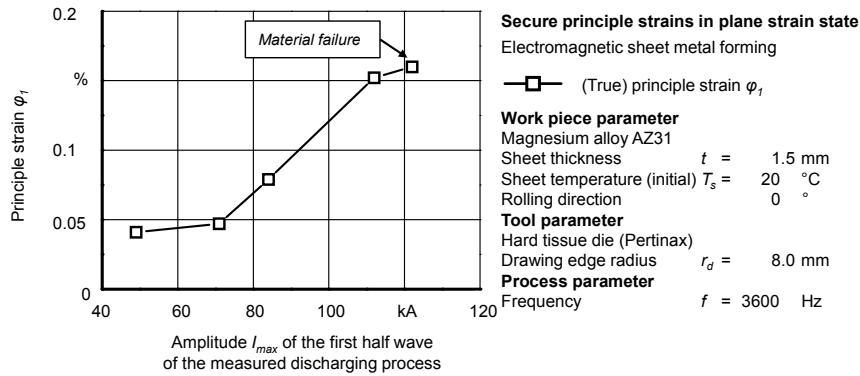


Figure 6: Experimentally measured principle strain  $\phi_1$

To decrease the principle strain  $\phi_1$  at the drawing edge  $r_d$  it is necessary to decrease the charging energy  $E$ . The influence of charging energy  $E$  or the tool coil current  $I_{max}(t)$  is shown in Fig. 7. Charging energy  $E = 6$  kJ leads to (true) principle strain  $\phi_1 = 0.15$ . There is no material failure expected at the drawing edge. Maximum (true) principle strain  $\phi_1$  at the cutting edge  $r_c$  is  $\phi_1 = 0.28$  which leads to material failure.

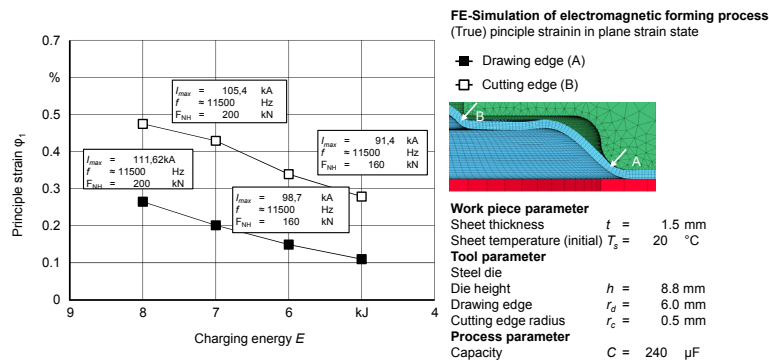


Figure 7: Principle strain  $\phi_1$  in dependence of charging energy  $E$  or tool coil current  $I(t)$

The corresponding work piece deformations are shown in Fig. 8. The forming process with charging energy  $E = 6$  kJ achieves a die filling of 78.7% with die height  $h = 8.8$  mm. The deviation from the targeted drawing edge  $r_d = 1.5$  mm at  $r_d = 6$  mm is about 75%. The deviation from the targeted work piece height  $h_w = 14.8$  mm to realizable heights  $h = 8.8$  mm is approximately 41%.

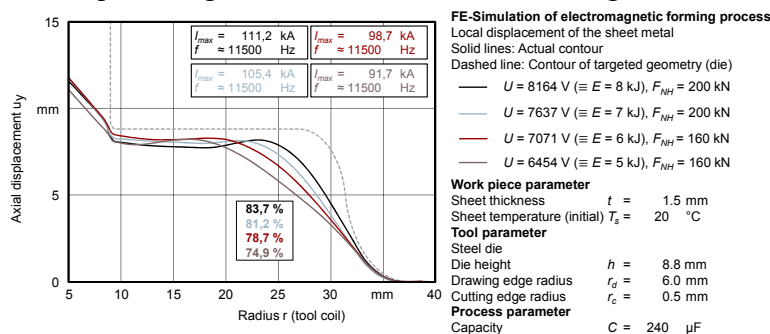


Figure 8: Displacement  $u_y$  for different charging energies  $E$  while drawing edge  $r_d = 6$  mm (simulation time = 300  $\mu$ s)

## 6 Conclusion

In the context of this paper, the process design using FE simulation for production of complex three-dimensional work piece geometry made of magnesium alloy AZ31 by electro-forming forming at room temperature was presented. For this purpose, in the first step a suitable simulation concept was developed. Within the framework of simulation an adjusted tool coil geometry as well as an adjusted blank holder has been identified. Depending on the charging energy defined blank holder forces has been determined.

By varying the die height  $h$ , the drawing edge radius  $r_d$  and the cutting radius  $r_c$  a suitable work piece geometry was identified without material failure. Die filling of 78.7 % was achieved. The deviation of the targeted work piece height  $h_w$  in relation to initial geometry is 41 %. The deviation of the targeted drawing edge  $r_d$  in relation to initial drawing edge  $r_d$  is 75 %

## Acknowledgement

The authors would like to thank the Arbeitsgemeinschaft industrieller Forschungsvereinigungen – AiF – (Federation of Industrial Research Associations) for funding this research within the project 18443 N1 .

## References

- El-Azab, A., Garnich, M., Kapoor, A., 2003. Modeling of the electromagnetic forming of sheet metals: state-of-the-art and future needs. *Journal of Materials Processing Technology* 142, pp. 744-754.
- Ahmad, I. R.; Shu, D. W., 2015: Experimental and Constitutive Study of Tensile Behavior of AZ31B Wrought Magnesium Alloy. *Journal of Engineering Mechanics* 141 (3), pp. 04014124.
- Bessonov, N., Golovashchenko, S., 2004. Numerical Simulation of Pulsed Electromagnetic Stamping Process. In: Kleiner, M. (Eds.), *High Speed Forming 2004, Proceedings of the 1st International Conference, Dortmund, Germany*.
- Cao, Q., Han, X., Lai, Z., Xiong, Q., Zhang, X., Chen, Q., Xiao, H., Li, L., 2015. Analysis and reduction of coil temperature rise in electromagnetic forming. *Journal of Materials Processing Technology* 225, pp. 185-194.
- Cazacu, O; Plunkett, B.; Barlat, F., 2006. Orthotropic yield criterion for hexagonal closed packed metals. *International Journal of Plasticity* 22 (7), pp. 1171-1194.
- Correia, J. P. M., Siddiqui, M. A., Ahzi, S., Belouettar, S., Davies, R., 2008. A simple model to simulate electromagnetic sheet free bulging process. *International Journal of Mechanical Science* 50, pp. 1466-1475.
- Cowper, G. R., Symonds, P. S., 1952. Strain-hardening and strain-rate effects in the impact loading of cantilever beams. Providence, Rhode Island, USA, Brown University, Division of Applied Mechanics, Technical Report No. 28.

- Doley, J. K.; Kore, S. D., 2014. FEM Study on Electromagnetic Formability of AZ31B Magnesium alloy. Huh, H.; Tekkaya (Eds.), Proceedings of the 6th International Conference, (ICHSF), Daejon, Korea, 2014, pp. 273-280.
- L'Eplattenier, P., Cook, G., Ashcraft, C., 2008. Introduction of an Electromagnetism Module in LS-DYNA for Coupled Mechanical Thermal Electromagnetic Simulations. Kleiner, M., Tekkaya, A.E. (Eds.), Proceedings of the 3rd International Conference (ICHSF), Dortmund, Germany, pp. 85-96.
- Feng, F., Huang, S., Meng, Z., Hu, J., Lei, Y., Zhou, M., Wu, D., Yang, Z., 2014. Experimental study on tensile property of AZ31B magnesium alloy at different high strain rates and temperatures. *Materials and Design* 57, pp. 10-29.
- Finckenstein, E. v., 1967. Ein Beitrag zur Hochgeschwindigkeitsumformung rohrförmiger Werkstücke durch magnetische Kräfte. Dissertation, Universität Hannover.
- Hahn, R., 2004. Werkzeuge zum impuls magnetischen Warmfügen von Profilen aus Aluminium- und Magnesiumlegierungen. In: Berichte aus dem Produktionstechnischen Zentrum Berlin, Hrsg.: Uhlmann, Dissertation, Technische Universität Berlin, Stuttgart: Fraunhofer IRB.
- Imbert, J. M., Winkler, S. L., Worswick, M. J., Oliveira, D. A., Golovashchenko, S., 2005. The Effect of Tool-Sheet Interaction on Damage Evolution in Electromagnetic Forming of Aluminium Alloy Sheet. *Journal of Engineering Materials and Technology* 127, pp. 145-153.
- Johnson, G. R., Cook, W. H., 1983. A constitutive model and data for metals subjected to large strain, high strain rates and high temperatures. Proceedings of the 7th International Symposium on Ballistics, Vol. 21, Den Haag, The Netherlands.
- Kurukuri, S., Worswick, M. J., Ghaffari Tari, D., Mishra, R. K., Carter, J. T., 2015. Rate sensitivity and tension - compression asymmetry in AZ31B magnesium alloy sheet. *Philosophical Transactions of the Royal Society* 327, p. 20130216.
- Lange, K., 1993. Umformtechnik, Band 4, Sonderverfahren, Prozeßsimulation, Werkzeugtechnik, Produktion. Heidelberg, New York, London: Springer.
- Mamalis, A. G., Manolakos, D. E., Kladas, A. G., Koumoutsos, A. K., 2006. Electromagnetic Forming Tools and Processing Conditions: Numerical Simulation. *Materials and Manufacturing Processes* 21, pp. 411-423.
- Meriched, A., Féliachi, M., Mohellebi, H., 2000. Electromagnetic Forming of Thin Metal Sheets. *IEEE Transactions on Magnetics* 36 (4), pp. 1808-1811.
- Neubauer, A., Strobe, H., Wolf, H., 1988. Hochgeschwindigkeitstechnologie der Metallbearbeitung. In: Berlin: VEB Verlag Technik.
- Oliveira, D. A., 2005. Electromagnetic forming of aluminium alloy sheet: Free-form and cavity fill experiments and model. *Journal of Materials Processing Technology* 170, pp. 350-362.
- Pérez, I., Aranguren, I., Gonzáles, B., Eguia, I., 2009. A new coupling method. *International Journal of Material Forming* 2 , pp. 637-640.
- Perzyna, P., 1966. Fundamental Problems in Viscoplasticity. *Advances in Applied Mechanics* 9, pp. 243-377.

- Psyk, V., Risch, D., Kinsey, B.L., Tekkaya, A.E., Kleiner, M., 2011. Electromagnetic forming – A review. *Journal of Materials Processing Technology* 211 (5).
- Ulacia, I., Imbert, J., Salisbury, C.P., Arroyo, A., Hurtado, I., Worswick, M.J., 2008. Electromagnetic Forming of AZ31B Magnesium Alloy Sheet: Experimental Work and Numerical Simulation. Kleiner, M.; Tekkaya, A. E. (Eds.), *Proceedings of the 3rd International Conference (ICHSF), Dortmund, Germany*, pp.191-200.
- Ulacia, I., Hurtado, I., Imbert, J., Salisbury, C.P., Worswick, M.J., Arroyo, A., 2009. Experimental and Numerical Study of Electromagnetic Forming of AZ31B Magnesium Alloy Sheet. *Steel Research International* 80 (5), pp. 344-350.
- Ulacia, I., Dudamell, N.V., Gálvez, F., Yi, S., Pérez-Prado, M. T., Hurtado, I., 2010. Mechanical behavior and microstructural evolution of a Mg AZ31 sheet at dynamic strain rates. *Acta Materialia* 58, pp. 2988-2998.
- Ulacia, I., Salisbury, C.P., Hurtado, I., Worswick, M.J., Arroyo, A., 2011. Tensile characterization and constitutive modeling of AZ31B magnesium alloy sheet over a wide range of strain rates and temperatures. *Journal of Materials Processing Technology* 211, pp. 830-839.
- Ulacia, I., Yi, S., Pérez-Prado, M., Dudamell, N., Gálvez, D., Letzig, D., Hurtado, I., 2012. Texture Evolution of AZ31 Magnesium Alloy Sheet at High Strain Rates. *Materials Science Forum*, pp. 706-709.
- Uhlmann, E., Scholz, M., 2003. Zerteilen von Aluminiumblechen durch Impulsmagnetfelder. Tagungsberichtsband zum „2. Kolloquium Elektromagnetische Umformung“, Kleiner, M. (Ed.), Dortmund, Germany.
- Uhlmann, E., Prasol, L., 2013. Holistic approach to pulse magnetic forming of magnesium alloy AZ31 at low forming temperatures. Archenti, A., Maffei, A. (Eds.), *Proceedings of the NEWTECH, Volume 2, Stockholm, Sweden*, pp. 9-24.
- Uhlmann, E., Prasol, L., Kawalla, R., Schmidt, C., Becker, T., 2014: Extension of formability of the magnesium wrought alloy AZ31B-O at room temperature by pulse magnetic forming. Huh, H.; Tekkaya (Eds.), *Proceedings of the 6th International Conference (ICHSF), Daejeon, Korea*, pp. 21-30.
- Unger, J., Stiemer, M., Schwarze, M, Svendsen, B., Blum, H., Reese, S., 2008. Strategies for 3D simulation of electromagnetic forming process. *Journal of Materials Processing Technology* 199, pp. 341-362.
- Wang, L., Chen, Z. Y., Li, C. X., Huang, S. Y., 2006. Numerical simulation of the electromagnetic sheet metal bulging process. *International Journal of Advanced Manufacturing Technology* 30, pp. 395-400.
- Winkler, R., 1973. Hochgeschwindigkeitsbearbeitung – Grundlagen und technische Anwendungen elektrisch erzeugter Schockwellen und Impulsmagnetfelder. VEG Verlag Technik Berlin.
- Zerilli, F. J.; Armstrong, R. W., 1985. Constitutive Equation for HCP Metals and High Strength Alloy Steels. *ASME Publications* 48, pp. 121-126.
- Xu, J. R., Cui, J. J., Lin, Q., Li, Y., Li C. F., 2015. Magnetic pulse forming of AZ31 magnesium alloy shell by uniform pressure coil at room temperature. *International Journal of Advanced Manufacturing Technology* 77 (1-4), pp. 289-304.